Through the Looking Sand:

A Study of Microwave Optics in Disordered Quartz Media

Nicholas McClure
PHYS 3304 – Intermediate Laboratory
Department of Physics and Astronomy,
Texas Tech University
(Dated: April 30, 2025)

Microwave radiation is a subset of electromagnetic radiation that exhibits similar wave properties to optical light, such as refraction and reflection. In this study, a plano-convex lens composed of quartz sand was placed in front of a Gunn oscillator microwave source of approximately (11 ± 1) GHz to investigate the angular dependence of incident and refracted waves and to test the Maxwell–Garnett prediction for sub-wavelength grains. A constrained linear fit of $\sin\theta_1$ versus $\sin\theta_2$ measurements yielded a refractive index of 1.497 ± 0.089 which differs by less than one standard deviation from the Maxwell–Garnett prediction (1.58 at $f = 0.62$). Additionally, the strong linearity of $\sin\theta_1$ vs. $\sin\theta_2$ confirms that Snell's Law governs refraction in this setup. These findings demonstrate that macroscopic optical models remain applicable in the microwave regime even when the dielectric medium possesses granular microstructure.

I. INTRODUCTION

The propagation of electromagnetic waves through a medium is governed by principles that are consistent across all regions of the EM spectrum. Microwave radiation, which has longer wavelengths than optical light, obeys principles such as refraction, reflection, interference, and transmission.[1, 2] This continuity allows microwave systems to serve as analogs for studying wave optics with high spatial resolution and accessibility.

Microwave optics refer to the use of microwave radiation to investigate wave phenomena typically associated with optical frequencies. These systems offer a macroscopic perspective for observing wave behavior that are familiar to the optical regime, such as beam focusing, diffraction, and polarization, which can all be demonstrated using larger, more easily manipulated components. This makes microwave optics an effective tool for research and pedagogical uses without the need for small-scale optical or interferometric components such as diffraction gratings or nanometer-scale slits.

In addition to testing this continuity, microwave studies of dielectric media both homogeneous and heterogeneous provide an opportunity to probe deeper material properties. Specifically, when the medium consists of granular materials and is largely heterogeneous such as quartz sand, effective medium theory predicts that the material will exhibit an averaged refractive index when the grain size is much smaller than the probing wavelength[3]. Despite local fluctuations in dielectric constant, a coherent wavefront can still propagate.

This study investigates the refraction of collimated microwave radiation through a plano-convex dielectric lens to explore both classical optical behavior and wave propagation in disordered granular media to determine the refractive index of the lensing material, and to investigate effective medium theory in the microwave regime.

II. THEORY

A. Snell's Law and Refractive Index

The interaction of electromagnetic waves with dielectric boundaries gives rise to reflected and transmitted fields governed by the continuity of the tangential components of the electric and magnetic fields. Consider a plane wave incident at an angle θ_1 on a planar boundary at $z = 0$ between two homogeneous, isotropic, and nonmagnetic media. The incident, reflected, and transmitted electric fields, polarized along $\hat{y}$, can be written as

$$\begin{aligned}
\mathbf{E}_i(x,z,t) &= \mathbf{E}_{0i}\cos(k_1 x\sin\theta_1 + k_1 z\cos\theta_1 - \omega t)\,\hat{y},\\
\mathbf{E}_r(x,z,t) &= \mathbf{E}_{0r}\cos(k_1 x\sin\theta_1 - k_1 z\cos\theta_1 - \omega t)\,\hat{y},\\
\mathbf{E}_t(x,z,t) &= \mathbf{E}_{0t}\cos(k_2 x\sin\theta_2 + k_2 z\cos\theta_2 - \omega t)\,\hat{y}. \quad (1)
\end{aligned}$$

At the boundary $z = 0$, continuity of the tangential electric fields requires phase matching:

$$\begin{aligned}
\mathbf{E}_i(x,0,t) &= \mathbf{E}_{0i}\cos(k_1 x\sin\theta_1 - \omega t)\,\hat{y},\\
\mathbf{E}_r(x,0,t) &= \mathbf{E}_{0r}\cos(k_1 x\sin\theta_1 - \omega t)\,\hat{y},\\
\mathbf{E}_t(x,0,t) &= \mathbf{E}_{0t}\cos(k_2 x\sin\theta_2 - \omega t)\,\hat{y}. \quad (2)
\end{aligned}$$

Phase continuity yields

$$k_1\sin\theta_1 = k_2\sin\theta_2, \quad (3)$$

and substituting $k = n\omega/c$ gives Snell's Law:

$$n_1\sin\theta_1 = n_2\sin\theta_2. \quad (4)$$

Importantly, Snell's Law holds independently of wavelength or intensity under the usual assumptions of isotropy and linearity[4].

B. Maxwell–Garnett Effective-Medium Model

For a heterogeneous or granular medium such as quartz sand, lens effective medium theory gives a macroscopic index. Using the Maxwell–Garnett equation[3, 5]:

$$\varepsilon_{\text{eff}} = \varepsilon_m \frac{(\varepsilon_i + 2\,\varepsilon_m) \;+\; 2\,f\,(\varepsilon_i - \varepsilon_m)}{(\varepsilon_i + 2\,\varepsilon_m) \;-\; f\,(\varepsilon_i - \varepsilon_m)}. \tag{5}$$

For $\varepsilon_i = 4.5$, $\varepsilon_m = 1.0$, and $f = 0.62$, we find that

$$\varepsilon_{\text{eff}} \approx 2.50, \qquad n_{\text{eff}} = \sqrt{\varepsilon_{\text{eff}}} \approx 1.58. \tag{6}$$

This experimental prediction of refractive index of granular media is what will be comparatively investigated in the Results section of this study.

Individual sand grains can scatter, but at a nominal frequency of (11 ± 1) GHz (wavelength $\lambda \approx 27\,\text{mm}$) versus a typical grain diameter $d \approx 0.2\,\text{mm}$,

$$\frac{d}{\lambda} \approx 0.007 \ll 0.1, \tag{7}$$

placing us firmly in the Rayleigh regime ($\sigma_s \propto d^6/\lambda^4$) where coherent refraction dominates. Mie–scattering corrections only become appreciable once $d/\lambda \sim 0.1$[6].

If dielectric loss were significant, the transmitted field would instead include an attenuation factor:

$$\mathbf{E}(z,t) = \mathbf{E}_0 e^{-\kappa z} e^{i(kz - \omega t)}. \tag{8}$$

C. Packing Fraction

An important assumption was made regarding the packing fraction value f. For prediction purposes, a value of $f = 0.62$ was chosen as this is the "working" packing fraction, typical for dry sand gently settled into a mold.

Random loose packing of uniform spheres has been measured at

$$f_{\text{RLP}} \approx 0.555\text{–}0.58 \quad [7], \tag{9}$$

whereas random close packing converges to

$$f_{\text{RCP}} \approx 0.636\text{–}0.64 \quad [8,\ 9]. \tag{10}$$

Polydisperse, angular natural sands such as quartz typically pack slightly less efficiently, with

$$f \approx 0.60\text{–}0.63 \quad [10]. \tag{11}$$

These frameworks explain why a coherent, refracted wavefront persists in quartz sand despite local dielectric fluctuations. Importantly, they demonstrate that classical optics properties that apply seamlessly in the microwave regime just as they do at optical frequencies, even within disordered granular media.

III. EXPERIMENTAL SETUP

A. Microwave Source and Detection

Coherent microwave radiation was generated using a Gunn diode oscillator operating at a frequency of approximately (11 ± 1) GHz. The output from the oscillator was coupled into a horn antenna, producing a collimated microwave beam directed along a linear optics bench. A plano-convex dielectric lens composed of finely ground quartz sand was positioned along the beam path, with the curved surface facing the source and the flat surface oriented toward a detection system. An electric field (E-field) probe connected to a multimeter set to detect voltage was placed approximately 60 cm beyond the lens to measure the transmitted intensity at various angles relative to the optical axis. on a large paper protractor affixed beneath the probe assembly was used to record angular positions. The angle of incidence θ_1 was defined as the angle between the incident beam and the normal to the flat surface of the lens, while the angle of refraction θ_2 was defined as the angle between the transmitted beam and the same normal.

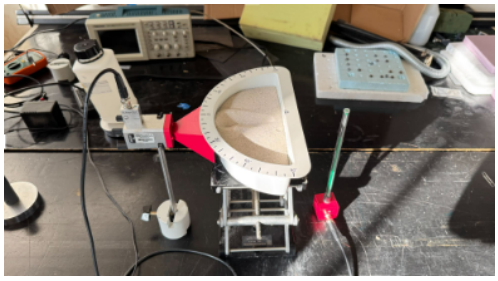

FIG. 1. Experimental setup showing Gunn oscillator and quartz sand lens

IV. PROCEDURE

A. Measurement Procedure

For each measurement, the horn antenna was rotated to achieve a specific angle of incidence θ_1, measured relative to the normal of the lens surface. At each fixed θ_1, the E-field probe was swept across the angular scale to locate the angle at which the detected voltage reached a maximum reading on the multimeter (i.e., when refracted radiation transversely reached maximum constructive interference), corresponding to the refracted beam. This angle was recorded as the refraction angle θ_2 with an uncertainty of $\pm 1°$. The multimeter provided strong variations in voltage, likely stemming from environmental effects or sub-optimal wave congruence. To collect a valid voltage reading, the multimeter was observed for 10 seconds, and the average voltage over that span of time was used.

B. Refractive Index Calculation

Five independent measurements were performed with θ_1 ranging from 10° to 45°, with each trial at a 10° separation. The recorded data were subsequently analyzed by plotting $\sin\theta_1$ versus $\sin\theta_2$, and performing a linear regression constrained through the origin. The slope of the resulting fit provided an experimental determination of the effective refractive index n_2 of the quartz sand lens.

V. RESULTS

A. Measured Refractive Index

Measurements of incident and refraction angles alongside detected voltages for five trials are presented in Table I. Uncertainties of $\pm 1°$ in angular measurements and $\pm 0.2\,\mathrm{V}$ in voltages are assigned based on instrumental precision. The refractive index n_2 for each trial is calculated using Snell's Law.

TABLE I. Measured angles, voltages, and calculated refractive indices with uncertainties.

Trial	θ_1 (deg)	θ_2 (deg)	Voltage (V)	$n_2 = \frac{\sin\theta_1}{\sin\theta_2}$
1	10 ± 1	7 ± 1	3.7 ± 0.2	1.42 ± 0.21
2	20 ± 1	13 ± 1	3.2 ± 0.2	1.52 ± 0.18
3	30 ± 1	18 ± 1	3.5 ± 0.2	1.62 ± 0.16
4	40 ± 1	24.5 ± 1	1.4 ± 0.2	1.55 ± 0.13
5	45 ± 1	30 ± 1	0.8 ± 0.2	1.41 ± 0.12

The trend of decreasing voltage with increasing refraction angle is shown in Figure 2. This decrease is attributed to beam divergence and partial internal reflection at higher angles.

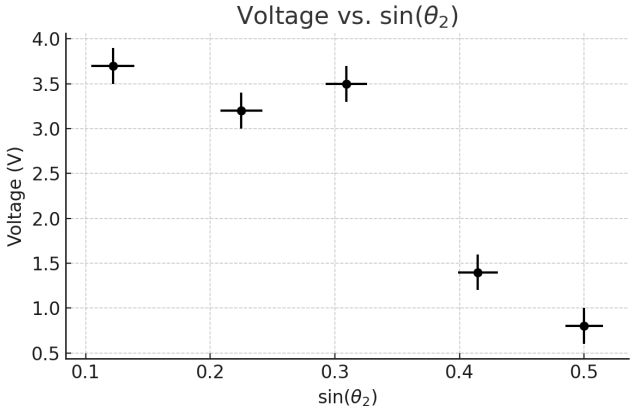

FIG. 2. Average Voltage vs. $\sin\theta_2$.

The effective refractive index was determined via linear regression of $\sin\theta_1$ versus $\sin\theta_2$, shown in Figure 3. A constrained linear fit through the origin yielded a slope corresponding to the refractive index. The residual fit, presented in Figure 4, demonstrates only slight deviations, supporting the linear model's validity.

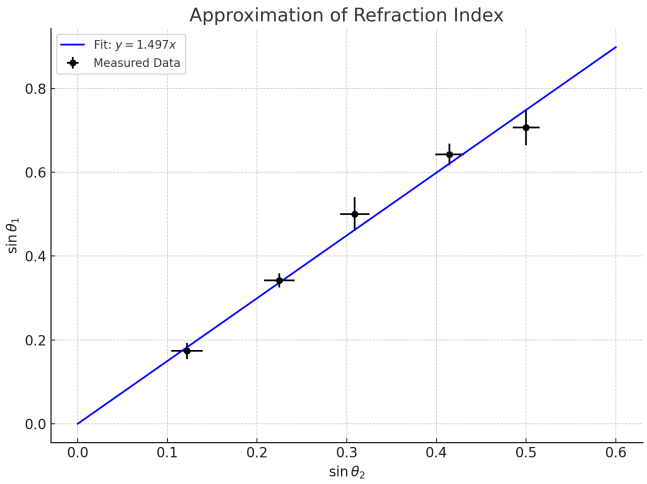

FIG. 3. Snell's Law Linear Fit: $\sin\theta_1$ vs. $\sin\theta_2$. The slope gives the estimated refractive index.

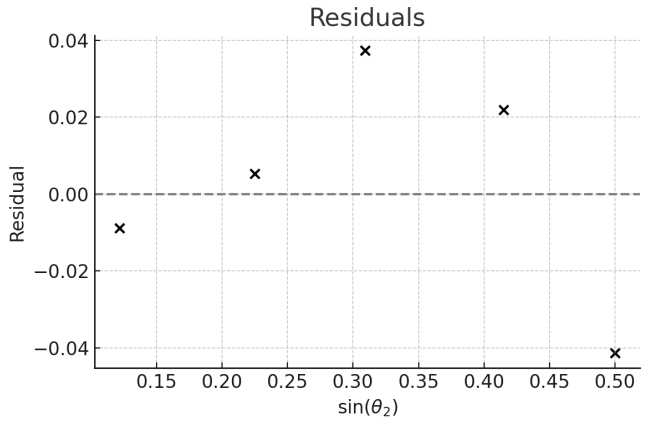

FIG. 4. Residuals of the linear fit, showing deviation of each data point from the model.

The slope of the fit yields a refractive index of $n_2 = 1.497 \pm 0.089$, with an associated p-value of 2.99×10^{-6} and R^2 value of .981, confirming a statistically significant fit. Uncertainties were propagated by combining experimental angular error ($\pm 1°$) and deviations from the linear model in quadrature. Voltage uncertainties were calculated from multimeter variations.

VI. DISCUSSION

A. Comparison with Literature Values

This study's refractive index value is in reasonable agreement with accepted values for crystalline quartz

reported by Malitson, where the ordinary and extraordinary refractive indices are approximately 1.5442 and 1.5533, respectively[11]. The measured value falls within experimental uncertainty of these reference values. Similarly, the experimental refractive index differs from the Maxwell–Garnett prediction of 1.58 by .933 standard deviations, showing statistical agreement with prediction. In contrast, comparison to other results in literature reveals modest variation across reported values, with a study by LEYBOLD Physics reported a refractive index of approximately 1.74 for a similar quartz sand system[12], which differs from the present result by approximately 2.73σ. The absence of reported uncertainties in the LEYBOLD study complicates direct comparison, but potential sources of discrepancy include variations in sand compaction, moisture content, grain size distribution, and differences in experimental alignment or measurement procedures. These factors could alter the effective dielectric constant of the medium, thereby influencing the observed refraction behavior and providing differing n_2 results. Additional studies on sand-based materials, such as lead-free glass manufactured from local sands in Thailand, have reported refractive indices ranging from 1.610 to 1.618 [13], while commercial quartz sand specifications cite values near 1.55 [14]. To provide a clearer comparison between the differences amongst these referenced results, Figure 5 presents a summary plot showing the deviations of each reference measurement from the experimental value in units of standard deviation.

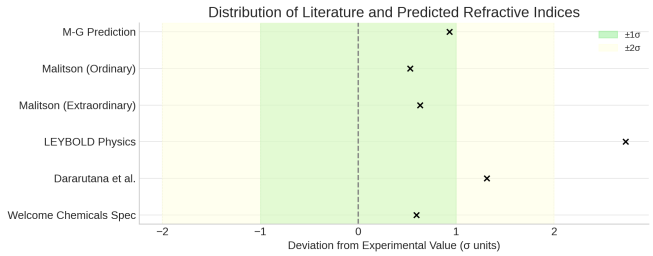

FIG. 5. Comparison of literature refractive index values to the measured refractive index, shown in units of standard deviation (σ).

B. Future Steps and Reccomendations

As seen in the summary plot, a majority of literature reported values for the refractive index of quartz sand is within one standard deviation of this study's result. However, a more precise measurement of the packing fraction f would allow for a higher level of accuracy in calculating the effective refractive index of our lens. Shown in equations 12 and 13, we see that packing fraction is directly related to volume and inversly related to density:

$$f = \frac{V_{\text{quartz}}}{V_{\text{total}}} \quad \propto \quad V_{\text{quartz}}, \tag{12}$$

$$f = \frac{m_{\text{sand}}}{\rho_{\text{quartz}}\, V_{\text{total}}} \quad \propto \quad \frac{1}{\rho_{\text{quartz}}}. \tag{13}$$

Future work can utilize these proportionalities to assist in collecting experimental values for f through Archimedes displacement, constraining the predicted value for n_2 and providing a more accurate benchmark for the study.

VII. CONCLUSION

Through the use of collimated microwave radiation passing through a granular quartz sand lens, this study measured an experimental quartz sand refractive index of 1.497 ± 0.089. This value is in significant agreement with predictions as well as literature values. Deviations from higher reported indices, such as the LEYBOLD Physics value of $n_2 = 1.74$, are likely attributable to experimental uncertainties including variations in grain packing density, moisture content, grain morphology, and alignment errors. These factors introduce deviations in the local dielectric environment that may not be captured by idealized theoretical models.

A strong linear correlation observed in the Snell's Law regression affirms that classical wave propagation theory remains valid within disordered granular dielectrics. The persistence of coherent refraction despite macroscopic heterogeneity highlights the robust nature of optical analogs in the microwave domain.

[1] NASA Radio JOVE Project, The properties of electromagnetic radiation, `https://tinyurl.com/radiojove-properties` (2000), accessed: 2025-04-10.

[2] OpenStax, The electromagnetic spectrum, `https://tinyurl.com/openstax-em-spectrum` (2016), accessed: 2025-04-10.

[3] A. Sihvola, *Electromagnetic Mixing Formulas and Applications* (The Institution of Engineering and Technology, 1999).

[4] D. M. Pozar, *Microwave Engineering*, 4th ed. (John Wiley & Sons, Hoboken, NJ, 2011).

[5] J. C. M. Garnett, Philosophical Transactions of the Royal Society of London. Series A **203**, 385 (1904).

[6] C. F. Bohren and D. R. Huffman, *Absorption and Scattering of Light by Small Particles* (Wiley, New York, 1983).

[7] G. Y. Onoda and E. G. Liniger, Physical Review Letters **64**, 2727 (1990).

[8] G. D. Scott and D. M. Kilgour, Journal of Physics D: Applied Physics **2**, 863 (1969).

[9] S. Torquato, T. M. Truskett, and P. G. Debenedetti, Physical Review Letters **84**, 2064 (2000).

[10] J. C. Santamarina, K. A. Klein, and Y.-H. Wang, *Soils and Waves: Particulate Materials Behavior, Characterization and Process Monitoring* (Wiley, New York, 2001).

[11] I. H. Malitson, Journal of the Optical Society of America **55**, 1205 (1965).

[12] LEYBOLD Didactic GmbH, *Refraction of Microwaves - P6.3.4.3*, LEYBOLD Physics Leaflets (2023), experiment manual accessed via Akbis Gazi University.

[13] P. Dararutana, S. Rattanadecho, and P. Wongchaiya, Physics Procedia **9**, 180–184 (2010).

[14] W. Chemicals, Quartz sand specification sheet, `https://www.welcomechemicals.com/quartz-sand-specifications` (n.d.), accessed: 2025-04-26.